Far-Field and Near-Field Distribution of GaN-Based Photonic Crystal LEDs With Guided Mode Extraction

Chun-Feng Lai, Jim-Yong Chi, *Senior Member, IEEE*, Hao-Chung Kuo, *Member, IEEE*, Hsi-Hsuan Yen, Chia-En Lee, Chia-Hsin Chao, Wen-Yung Yeh, and Tien-Chang Lu

Abstract—The near-field and far-field distribution of GaN LEDs with square photonic crystal (PhC) lattice are experimentally investigated. The optical images of the near-field pattern are obtained from the guided electroluminescent light generated at the center of a special annular structure. For increasing lattice constant, symmetric patterns with varying number of petals according to the symmetry of the PhC are observed. The far-field distribution is studied with GaN-based film-transferred PhC LEDs with the thickness about 1500 nm. Angular-resolved measurements under electrical injection revealed guided modes extraction behavior and polarization based on the Bragg's diffraction with the PhC lattice. Good agreement with the two-dimension free photon band structure is obtained.

Index Terms—GaN, LEDs, photonic crystal (PhC).

I. INTRODUCTION

THROUGH the Bragg diffraction with the photonic crystal (PhC), guided light in PhC LED chips can escape from the deleterious trapping effects due to total internal reflection [1]–[7]. Aperiodic PhC patterns have been reported for isotropic light extraction [6]. For controlling the collimation and polarization properties, periodic PhC with anisotropic light extraction has also been reported [4], [5], [8]. In this study, a detailed investigation was conducted to gain insights for the near-field and the far-field distribution of the guided mode extraction from the GaN-based PhC LEDs under electrical injection. A direct imaging approach is used for the in-plane angular distribution of the extracted light in the near field using an annular structure under electrical injection [2], [3]. The far-field patterns are investigated with the angular-resolved electroluminescence (EL) spectroscopy technique using a film-transferred LED structure under the electrical injection. The experimental results are compared with the band structure calculation. In addition, angular distribution is also examined in the polarization-resolved
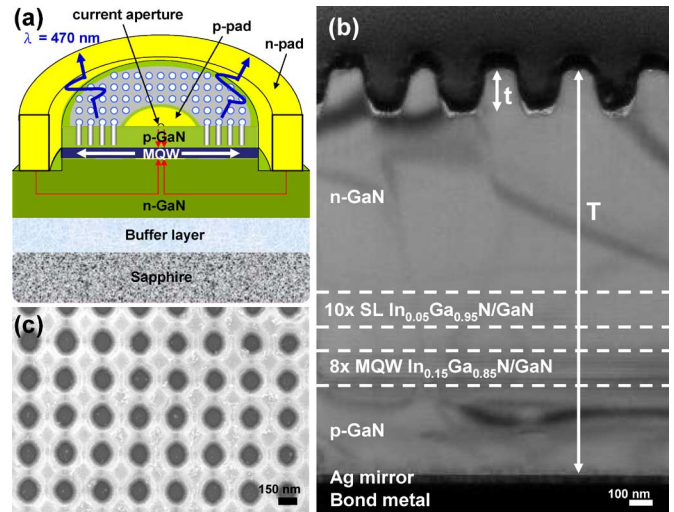
Fig. 1. Near-field and far-field sample structures. (a) Schematic diagram of the GaN-based blue LED structure with annular PhC region. (b) Cross-sectional TEM micrograph of a film-transferred GaN PhC LED structure with the etch depth $t = 150$ nm and GaN cavity thickness $T = 1500$ nm. (c) Top-view SEM image of PhCs on film-transferred LED with the lattice constant $a = 350$ nm and the diameter of air holes $d = 200$ nm fabricated with the holographic lithography.

manner. It is found that the emitted lights that are collinearly coupled to the reciprocal lattice are strongly TE polarized, while the noncollinearly coupled modes can posses both TE and TM polarization. The complicated polarization pattern dependence of the PhC extracted light will have different reflection properties from the conventional light sources that need to be understood especially for illumination applications.

II. EXPERIMENTS

A. Sample Preparation

For near-field study, a special structure is used, as shown in Fig. 1(a). The GaN-based LED samples used in this study were grown by metal–organic chemical vapor deposition (MOCVD) on a c-axis sapphire (0 0 0 1) substrate. The LED structure (dominant wavelength λ at 470 nm) was composed of a 1-μm-thick GaN bulk buffer layer on c-sapphire substrate, a 2-μm-thick bottom n-GaN current spreading layer, a 100-nm-thick InGaN/GaN-active region consisting of multiple quantum wells (MQWs), and a 130-nm-thick top p-GaN current spreading layer. An annular region of square PhC lattice with an inner/outer diameter of 100/200 μm was patterned by holographic lithography. Two different periods of the lattice constant, 260 and

410 nm, are used for the near-field study. The holes were then etched into the top p-GaN layer using inductively coupled plasma (ICP) dry etching to a depth $t = 120$ nm. The electron-beam-evaporated Ni/Au film (10/5 nm) was used as the transparent ohmic contact layer (TCL) to p-GaN and a 200-nm-thick SiO_2 layer for passivation. The Ti/Al/Ti/Au (100/1000/100/2000 nm) deposited on the smooth surface of n-type GaN, which was protected during the lithography process to serve as the n-type electrode. Finally, Ti/Al/Ti/Au (100/1000/100/2000 nm) layer was deposited onto TCL as the p-type electrode on LEDs.

For the far-field study, the employed LED structure consists of a 30-nm-thick GaN nucleation layer, a 4-μm-thick undoped GaN buffer layer, a 3-μm-thick Si-doped n-GaN layer, which consists of a 150 nm $In_{0.05}Ga_{0.95}N$/GaN superlattice (SL) with 10 periods, a 120 nm $In_{0.15}Ga_{0.85}N$/GaN MQW active region (dominant the wavelength $\lambda = 470$ nm) with eight periods, a 20-nm-thick Mg-doped p-AlGaN electron blocking layer, a 300-nm-thick Mg-doped p-GaN contact layer. The detailed wafer processing of thin-film GaN LEDs associated PhC is the same as in [9], [10] using the laser lift-off technique to remove the growth substrate. The resulting structure is then thinned down by chemical–mechanical polishing (CMP) to obtain the GaN cavity thickness around 1500 nm. The PhC with a square lattice of circular holes was then defined by holography lithography. Holes were etched into the top n-GaN surface to a depth $t = 150$ nm. Fig. 1(b) shows the thin-film GaN PhC LED structure cross section of the transmission electron microscopy (TEM) image. The lattice constant a of PhC used for the far-field study is 290, 350, and 400 nm, and the hole diameter d is 200 nm. A scanning electron microscopy (SEM) image of the square lattice PhC structure is shown Fig. 1(c). Finally, a patterned Cr/Pt/Au (30/70/2000 nm) electrode was deposited on n-GaN as the n-type contact layer and Cr/Au (30/2000 nm) metal was deposited on Si substrate backside.

B. Experimental Setup

The schematics for the experimental setup are shown in Fig. 2(a) and (b) for near field and far field, respectively. An EL probe station system is utilized for the near-field experiment after fabrication, which included continuous wave (CW) current source (Keithley 238), a 15× microscope objective with numerical aperture (NA) = 0.32. A 15× UV objective with NA of 0.32 is used to collect the on-axis emission signal from the sample and formed a high-resolution image on a charge-coupled device (CCD) and recorded with a digital camera. An example of the observed image is shown in the inset.

The angular-resolved measurement under electrical current injection was performed to study the far-field distribution using a setup as shown in Fig. 2(b). A continuous current 20 mA was injected into the GaN film-transferred PhC LEDs packaged in transistor outline (TO) cans at room temperature. The light emission spectra were taken for every zenithal angle with 0.2° resolution from −90° to +90°. These spectra are then displayed on a wavelength versus angular plot with the color of the pixel
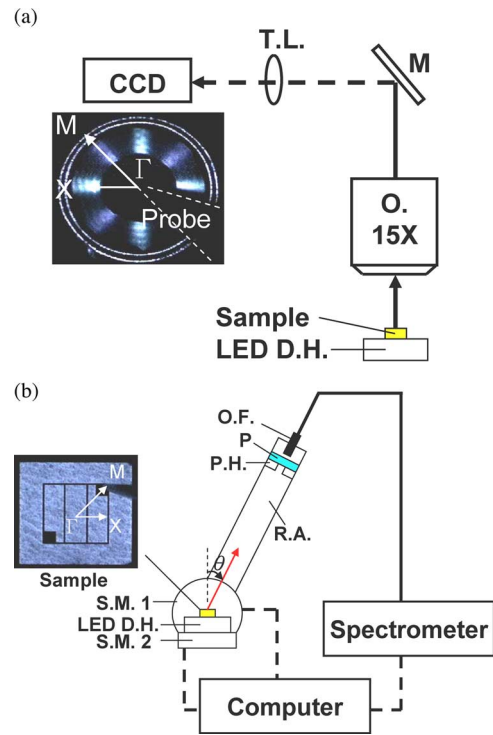

Fig. 2. (a) EL probe station and CCD imaging system setup, where D.H.: driver holder; M.: mirror; T.L.: tube lens; O.: objective. (b) Angular-resolved system setup, where S.M.: step motor; R.A.: rotating arm; P.H.: pinhole; P: polarizer; O.F.: optical fiber. Light emitted at the polar angle of θ, defined with respect to the direction normal to the sample surface, collected by optical fiber with a pinhole (diameter 1 mm) and a polarizer, which was placed at a distance of 15 cm from the sample. The sample was mounted on a rotating step motor 2 in order to find the correct in-plane direction from $\Gamma-X$ to $\Gamma-M$.

representing the intensity of the spectra color-coded according to a scale bar. Spectra are collected along the $\Gamma-X$ and $\Gamma-M$ directions. The polarized spectra are then taken with the polarizer oriented in s- and p-directions.

III. RESULTS AND DISCUSSION

Many different structures of PhC have been proposed and investigated for various ways to tailor the beam properties for particular applications. We investigated the square lattice because it is simple, retains the 2-D features, and is a model system for other slab structures. It is also the lattice structure that favors the polarized light emission [5]. The angular-resolved spectroscopic technique is a powerful method to investigate the quasiresonant modes that lie above the light lines to extract the waveguided lights. These quasiresonance modes are particularly important to assist the waveguided light to escape from LED chips [11].

A. Near Field

Using the annular sample structure shown in Fig. 1(a), the angular distribution of the near-field emission in the plane of the waveguide can be directly imaged. The details have been described before [3], only a brief discussion is given here.

The extraction of waveguided EL light into air can be described by the relation $|k + G| < k_0$, where k is wave vector
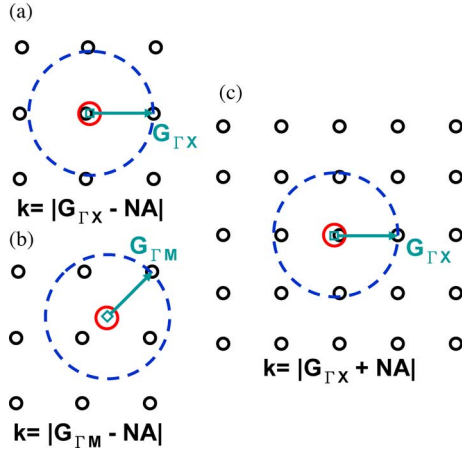
Fig. 3. Ewald construction for a/λ increases above the cutoff and just start to couple with the shortest lattice vector $G_{\Gamma X}$ (a) in the $\Gamma - X$ directions. (b) $\Gamma - M$ direction with the resultant wave vector falling outside the NA circle and will not be seen by the NA $= 0.32$ objective. (c) a/λ increases further as nk_0 just starts to leave the NA circle to disappear from the CCD image. The solid circles are the NA cone and the dash circles are the waveguided mode cone.
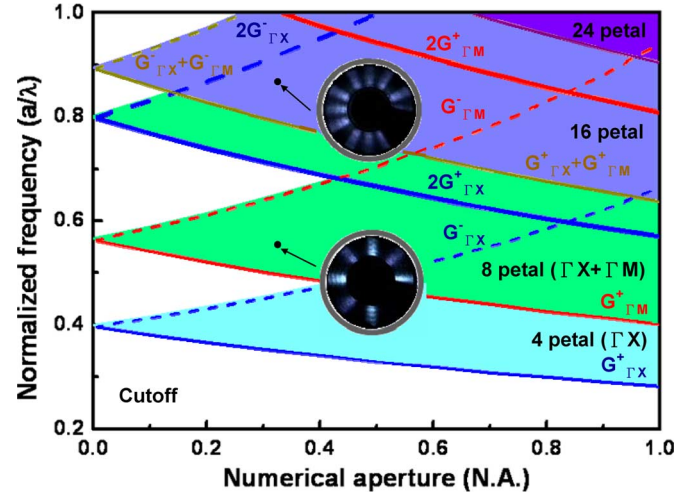

Fig. 4. Maps showing regions with different number of petals. The formula on the right of the figure is the boundary for regions. The insets showed the observed eightfold ($a = 260$ nm) and 16-fold ($a = 410$ nm) symmetry patterns. The regions of various petals are shown with different gray levels (color online). The directions of the petals are shown in the parenthesis. The "+" and "–" signs indicate the lower and upper boundary for the regions. The effective index used to generate the curves is $n = 2.5$.

of light and G is a reciprocal vector. For extraction into a cone with half angle θ, the relation is $|k + G| < $ NA, where NA $= \sin \theta$ and θ is the acceptance angle for the objective lens to collect the emitted light. For the present PhC structure, such a relation can be represented graphically with the Ewald construction projected on the waveguiding plane. An example of the Ewald construction is shown in Fig. 3. The two circles in each figure correspond to the waveguide mode circle (dashed blue) with radius $k = 2\pi n_{\text{eff}}/\lambda$ at the outside, where n_{eff} is the effective refractive index of the guided wave; and the NA circle with radius NA $= 0.32k_o$ in the middle (red). When the in-plane component of the resultant wave vector, after coupling to a reciprocal lattice vector, falls inside the NA circle, the diffracted light can escape into air and can be picked up with the objective lens.

As shown in Fig. 3, as a/λ increases above the cutoff, the guided wave vector can couple with increasing number of reciprocal points. The increased coupling possibilities are observed as the increased number of petals in the images.

For $k > G_{\Gamma X}$, the wave vector will start to couple with the nearest neighbors lying at $G_{\Gamma X}$ away and the resultant wave vector falls inside the NA circle, as shown in Fig. 3(a). But for the $\Gamma - M$ direction, the resultant wave vector fall outside the NA circle and will not be seen by the NA $= 0.32$ objective [Fig. 3(b)]. Therefore, a pattern with four petals pointing in the $\Gamma - X$ direction is observed. As a/λ increases further, the resultant wave vector after coupling to $G_{\Gamma X}$ may fall short of the NA circle and will not be observed [Fig. 3(c)]. Thus, there is a range of a/λ within which the resultant wave vector can fall into the NA circle for a particular propagation direction. The boundary for this range in the $\Gamma - X$ direction can be determined by the relation $k = |G_{\Gamma X} - \text{NA}|$ to be $a/\lambda = 1/(n + \text{NA})$. When a/λ increases further to the situation as shown Fig. 3(c), the resultant wave vector will leave the NA circle. In this case, $k = |G_{\Gamma X} + \text{NA}|$ and $a/\lambda = 1/(n - \text{NA})$.

For $k > G_{\Gamma M}$, the coupling to second nearest neighbor, lying at $G_{\Gamma M}$ from the center, becomes possible and four more petals appear corresponding to four equivalent $\Gamma - M$ directions. For even larger lattice constants, coupling to the points lying at $G_{\Gamma X} + G_{\Gamma M}$ away is possible and the number of petals increases to 16. The boundary separating the regions with different number of petals depends and NA can be derived using the Ewald construction. The regions with different number of petals can be readily derived and is shown with different colors in Fig. 4 along with the examples of the observed CCD images.

The earlier discussion considers the simple case of single-mode propagation in the waveguide plane. Since the thickness of the epitaxial layer used for this study is 3 μm, the waveguiding is multimode. Every mode of these multimodes can couple with different reciprocal vectors to form their own boundaries for a given number of petals. When plotted on the map, these boundaries will appear as a ribbon of lines. Since, in reality, only a few modes out of the whole multimode ensemble are seen, for simplicity, only the case for one mode is shown in Fig. 4.

B. Far Field

Far-field distribution of light sources is important for many applications. In PhC LED, the far-field distribution will be significantly modified by the PhC diffraction. The waveguided light traveling in the plane of wafer will be diffracted by the reciprocal wave vectors associated with the PhC. Due to the discrete nature of the waveguide modes, these diffracted light will exhibit anisotropy in the far-field pattern both in the zenith direction and the Azimuthal direction. In this study, the anisotropy in two high symmetry directions over a large range of a/λ was measured and discussed in the context of the band structure.

Fig. 5 shows the band structure for the TE modes in the present slab waveguide in the free photon limit with $n = 2.5$. Only
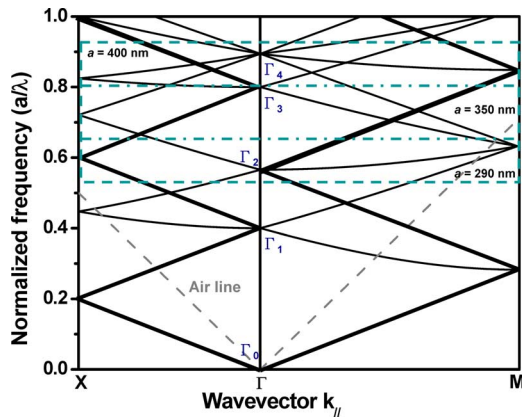
Fig. 5. Free photon band structure calculated with $n = 2.5$ for the TE modes. The thick lines indicate the collinear coupled bands. The thin lines indicated the noncollinear coupled bands. The boxes indicating the regions observed in this study with $a = 290$, 350, and 400 nm. The high symmetry points along the Γ-axis are labeled as Γ_0 through Γ_4.

Fig. 6. Angular-resolved spectra without polarizer for lattice constant (a) $a = 290$ nm, (b) $a = 350$ nm, and (c) $a = 400$ nm, where $\Gamma-X$ direction points to the left and $\Gamma-M$ direction points to the right.

the TE modes are considered, since the present MQW structure generates TE-polarized light propagating in the waveguide plane due to the valence band mixing of the QW light emission [12], [13]. Three different a values, 290, 350, and 400 nm, and the spectra spread of the present MQW sample, full-width at half-maximum (FWHM) = 50 nm, create a range of $u = a/\lambda$ from 0.53 to 0.92 for experimental investigation, as enclosed in the boxes shown in Fig. 5. The air lines are shown as dashed lines. Above the air lines, the band structure exhibits an abundance of resonant states that will be involved in the PhC-assisted light extraction. Using the angular-resolved spectroscopic technique, most of these states can be investigated efficiently. Fig. 6(a)–(c) shows the spectra taken along the $\Gamma-X$ (left) and $\Gamma-M$ (right) directions in unpolarized state for $a = 290$, 350, and 400 nm, respectively. These data can be transformed into dispersion curves to be compared with the calculated band structures shown in Fig. 5 that serves as a useful framework for the understanding of the experimental results. To examine the polarization of the spectra, a polarizer is used in front of the spectrometer with the polarization axis in the s- or p-orientation and the spectra retaken. It is found that certain lines are strongly polarized while the others have a mixed polarization. Due to the shallow etching of the present sample that results in a negligible narrow bandgap, the observed dispersion in this study was in good agreement with the calculated free photon band. The band structure shown in Fig. 5 essentially consists of bands emanating from four symmetric points labeled as Γ_1 through Γ_4 on the Γ-axis in $\Gamma-X$ and $\Gamma-M$ directions. These bands are formed by the collinear and noncollinear coupling with the reciprocal vectors $G_{\Gamma X}$, $G_{\Gamma M}$, $G_{\Gamma X \Gamma X}$, and $G_{\Gamma X \Gamma M}$, respectively. The thick lines marked the collinearly coupled bands, the rest of the bands are noncollinearly coupled bands. It will be shown that, for the present MQW samples, the collinearly coupled bands are singly degenerate and possess strong TE polarization. The noncollinearly coupled bands are doubly degenerate and have mixed polarization state.
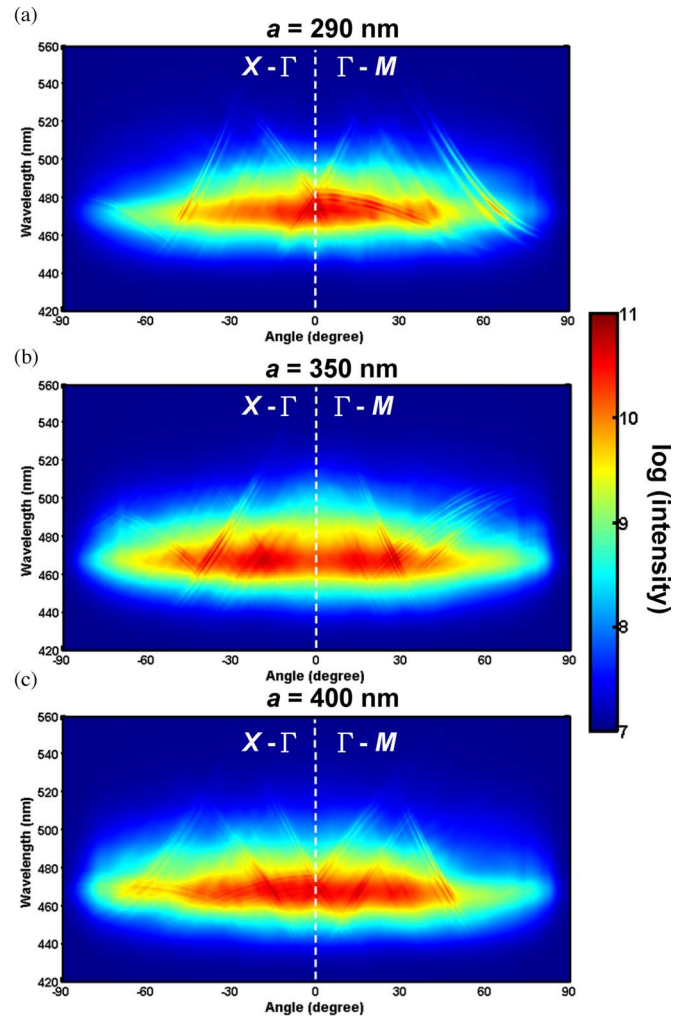
To serve as an example for others, the case for $a = 290$ nm will be discussed in more detail. Fig. 6(a) shows the angular-resolved spectra taken from $-90°$ to $90°$ with an accuracy of $0.2°$. It is found to be symmetrical around the vertical directions and consists of many sharp lines superimposed on the broad and diffuse Fabry–Perot background. The symmetry of the distribution is a reflection of the present electrical current injection in which the recombination light radiates isotropically in the Azimuthal MQW plane. The narrow lines are the waveguide mode lines that are diffracted by the PhC s. The spectra are taken along the symmetric $\Gamma-X$ and $\Gamma-M$ directions after careful alignment. Only 4–6 modes are seen despite a total of 15 available modes for the waveguide based on the index profile shown in Fig. 1(b). The reasons may be the nonuniform coupling to the waveguide modes due to the uniform carrier distribution, and different electric field overlap with the quantum wells among others.

The $a = 290$ nm lattice corresponds to $u = 0.53$–0.65 covering the Γ_2 point. Fig. 8(a) shows the corresponding band structure of the spectra after making the transformation of the
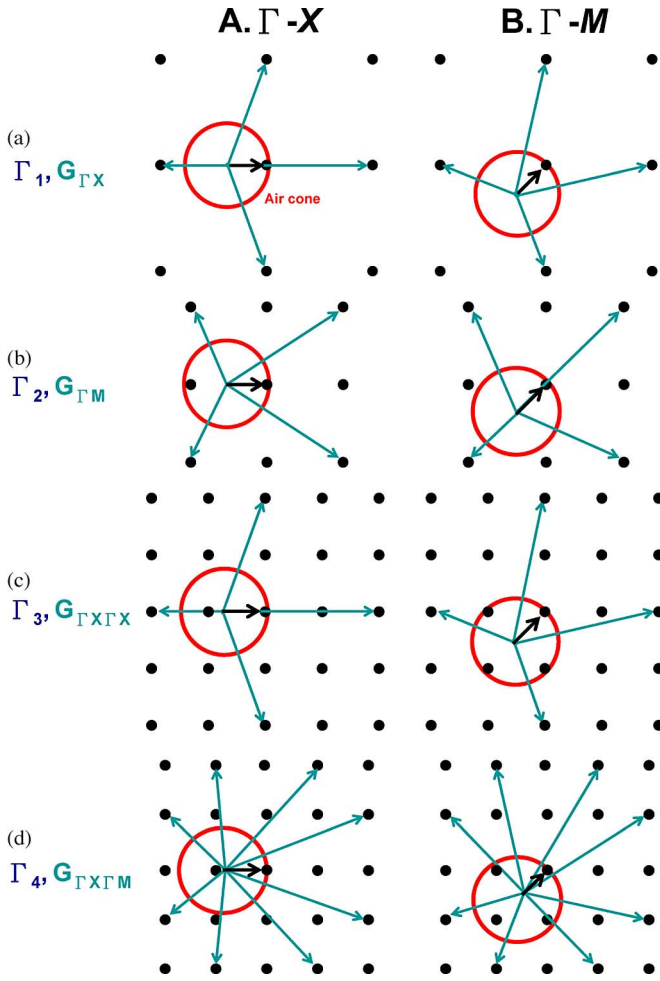
Fig. 7. Coupling diagram at (a) Γ_1, (b) Γ_2, (c) Γ_3, and (d) Γ_4 with $G_{\Gamma X}$, $G_{\Gamma M}$, $G_{\Gamma X \Gamma X}$, and $G_{\Gamma X \Gamma M}$, respectively. The column A indicates the wave vector coupling in the $\Gamma-X$ direction and column B, the $\Gamma-M$ direction. The red solid circles are the air cone. The thick arrows and thin arrows are the wave vectors.

Fig. 8. (a) Mode dispersions for $a = 290$ nm taken without the polarizer. The superimposed lines are the free photon band diagram with the solid lines corresponding to the singly degenerate band and dashed lines indicate doubly degenerated band. (b) and (c) Mode dispersion with the s- and p-polarization.

data shown in Fig. 6(a) with $k// = a \sin \theta/\lambda$. It can be seen that the band structure in this range consists of two bands emaciating from the Γ_2 in the $\Gamma-X$ direction and three in the $\Gamma-M$ direction. An examination of the polarized images shown in Fig. 8(b) and (c) reveals that the two bands in the $\Gamma-X$ direction possess mixed polarization. For the three bands in the $\Gamma-M$ direction, the outer two bands of the three bands show strong TE polarization while the middle band with less dispersion has mixed state of the polarization. The reason for the mixed polarization is due to the symmetric and antisymmetric coupling of the two degenerate states of this band as a result of the noncollinear coupling with the reciprocal wave vectors that results in a pseudo-TM mode [14], [15]. As shown in Fig. 7(b), Γ_2, for the modes traveling in the $\Gamma-M$ directions, there are three bands resulted from coupling with the four equivalent $G_{\Gamma M}$ wave vectors pointing in four equivalent $\Gamma-M$ directions. Two of the $G_{\Gamma M}$ wave vectors are collinear with the $\Gamma-M$ direction. The other two are lying perpendicular to the $\Gamma-M$ direction to provide noncollinear coupling with the modes propagating in the $\Gamma-M$ direction. The noncollinear coupling forms the
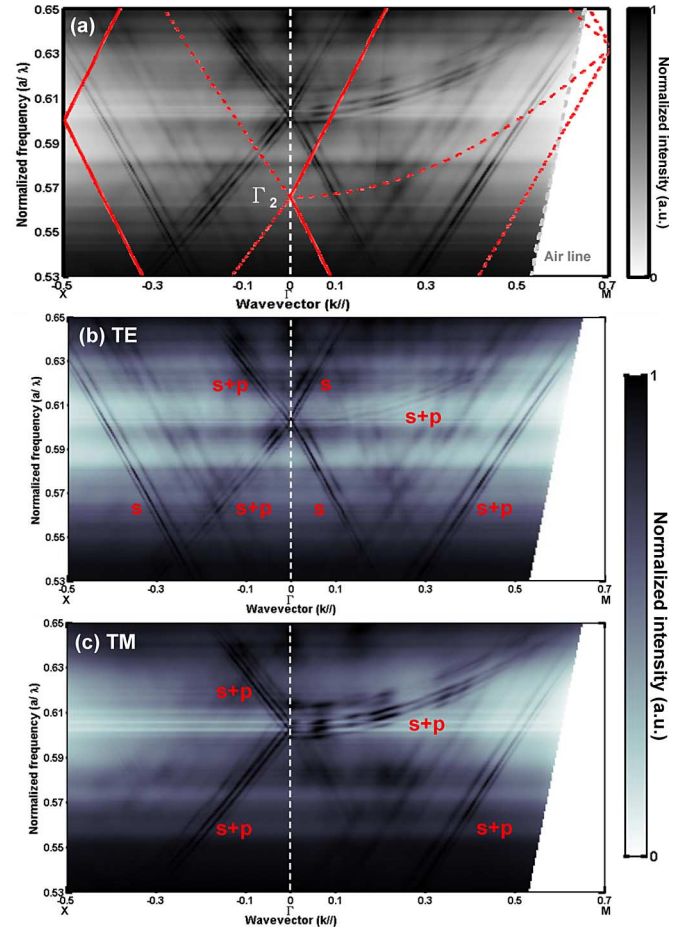
doubly degenerate band while the collinearly coupled band is singly degenerate. Fig. 8 (b) and (c) shows that the two strongly dispersed bands in the $\Gamma-M$ directions are only observed in the s-polarized image indicating that the bands are TE-polarized. While the middle band is seen in both the s- and p-orientations indicating that they have a mixed polarization. For the $\Gamma-X$ direction the modes can be noncollinearly coupled to the four equivalent wave vectors, $G_{\Gamma M}$'s and resulted in two doubly degenerate bands (Fig. 7(b), Γ_2, B). The two degenerate states in each band are reduced to the symmetric and antisymmetric coupled states with the E field running perpendicular and parallel to the propagation direction, respectively. The symmetric coupled bands will have TE polarization, while the antisymmetric coupled bands will have TM polarization. In addition to these mode lines, two other families of lines, entering from below and pointing away from Γ-axis, appear in Fig. 8. They are part of the lines emanating from Γ_1 lying below. The bands emanating from this point are actually formed in the same manner as that of Γ_2, except that the coupling reciprocal wave vector is with the $G_{\Gamma X}$'s (Fig. 7(a), Γ_1, A and B). Collinear and noncollinear coupling with $G_{\Gamma X}$'s result in the three bands emanating toward the X point, while two bands are pointing toward M point, reversing
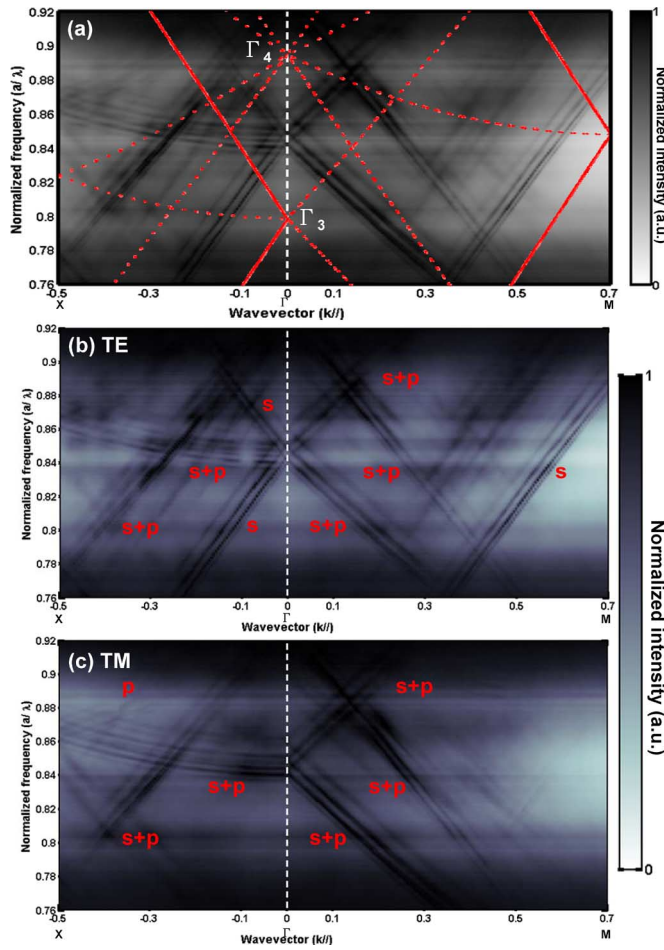
Fig. 9. (a) Mode dispersions for $a = 400$ nm taken without the polarizer. The superimposed lines are the free photon band diagram with the solid lines corresponding to the singly degenerate band and dashed lines indicate doubly degenerated band. (b) and (c) Mode dispersion with the s- and p-polarizations.
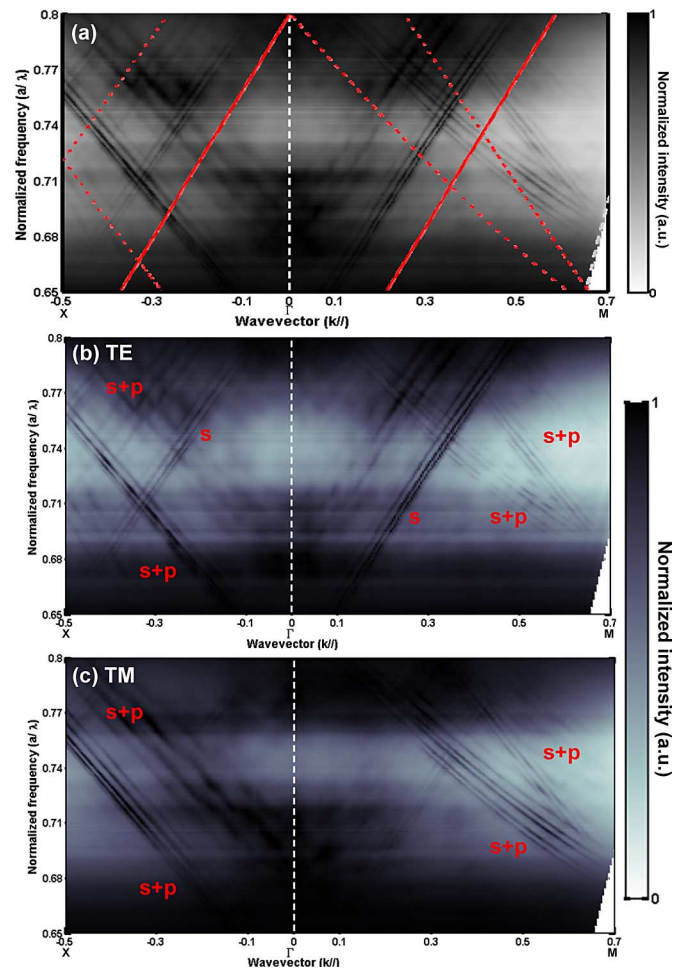

Fig. 10. (a) Mode dispersions for $a = 350$ nm taken without the polarizer. The superimposed lines are the free photon band diagram with the solid lines corresponding to the singly degenerate band and dashed lines indicate doubly degenerated band. (b) and (c) Mode dispersion with the s- and p-polarizations.

that for the Γ_2 point. The noncollinearly coupled mode lines entered the image from the bottom in the $\Gamma - M$ sector of Fig. 8 and exhibit a mixed polarization while the collinearly coupled mode lines appear in the $\Gamma - X$ sector have the TE polarization.

The experimentally observed bands appear to be shifted away from the calculated lines. The bands are also appeared to be shifted from sample to sample when displayed in the present scale. There are several factors causing the shifts. Due to the shallow PhC, the field of low-order modes has poor overlap with the PhC and will not been extracted, hence the low-order modes with effective indexes close to that used for the calculated lines are missing. In addition, the thickness of the sample also varies by 100–200 nm due to the sample tilting during lapping and thinning to cause an uncertainty in the thickness of the waveguide. Such a variation will cause a corresponding shift in the effective indexes for the waveguiding modes, which in turn cause the mismatch of the bands from sample to sample. Taking these factors into account the agreement between the experiment and calculation are reasonably good.

For the Γ_3 point, the band structure resembles that at Γ_1, but the wave vectors involved here have the length of two $G_{\Gamma X}$.

The a/λ is also twice that at Γ_1, thus the bands appears to be identical to those at Γ_1 except that they are shifted up to the Γ_3 point, as shown in Fig. 9. The polarization for each of the bands is also the same as that of Γ_1. In addition to the bands emanating from the Γ_3 point, there are some bands that come from the Γ_4 point lying above shown in Fig. 10. The Γ_4 point is different from Γ_1, Γ_2, and Γ_3. There are four bands, instead of three and two, at Γ_2 and Γ_3, respectively, emanating from this point for both directions. An analysis indicates that these bands actually result from the eight equivalent $G_{\Gamma X \Gamma M}$'s for the Γ point (Fig. 7(d), Γ_4, A and B). For the $\Gamma - X$ directions these eight vectors arranged in four symmetric pairs that can noncollinearly couple to the k vectors to form four double degenerate bands. For the $\Gamma - M$ directions, there are also four such pairs that can couple to the k vectors and resulted in four bands that are emanating from the Γ_4 point. These two groups of four bands are all doubly degenerate and posses mixed polarization. The two lowest bands from the two groups are seen in Fig. 9(a) (one of them barely visible). The two bands entering the image field from above and pointing away from the Γ-axis in either

direction appear in both polarizations, as shown in Fig. 9(b) and (c).

Fig. 10 depicts the band structure that appeared in the $a = 350$ nm lattice. It mainly consists of bands that are emanating from Γ_2 point lying below and the Γ_3 and Γ_4 points lying above. The polarizations of these modes are in agreement with the discussion shown earlier. However, it should be noted that at the crossover point away from the Γ-axis, the anticrossing formed by the two bands is not observed due to the present shallow etching [12].

IV. Conclusion

Experimental investigation of the near-field and far-field distribution has been conducted on GaN LEDs with square PhC lattice. The near-field distribution, studied in the Azimuthal direction with a specially designed waveguide structure, shows a symmetric pattern with varying number of petals in the plane of the waveguide. The regions corresponding to varying number of petals are determined for increasing lattice constant. The far field was studied with GaN-based film-transferred PhC LEDs with the GaN thickness about 1500 nm. Angular-resolved measurements under electrical injection revealed guided modes extraction behavior based on the Bragg's diffraction with the lattice. Due to the shallow etching of the present case, the dispersion curve of the mode lines observed in the angular-resolved spectra closely resemble the band structures of the free photon band with the index corresponding to the average index for the slab waveguides. Polarization of the emitted lines has also been studied and a dependence of the polarization on the collinear or noncollinear coupling with the reciprocal wave vectors was observed. Good agreement with the 2-D free photon approximation was obtained. The present results indicate that the PhC-enhanced LED will have complicated polarization distribution that will have implication for the use of these LEDs as the light sources for display and lighting.

Acknowledgment

References

[1] M. R. Krames, O. B. Shchekin, R. Mueller-Mach, G. O. Mueller, L. Zhou, G. Harbers, and M. G. Craford, "Status and future of high-power light-emitting diodes for solid-state lighting," *J. Display Technol.*, vol. 3, pp. 160–175, 2007.

[2] C. F. Lai, H. C. Kuo, C. H. Chao, H. T. Hsueh, J.-F. T. Wang, W. Y. Yeh, and J. Y. Chi, "Anisotropy of light extraction from two-dimensional photonic crystal light-emitting diodes," *Appl. Phys. Lett.*, vol. 91, pp. 123117-1–123117-3, 2007.

[3] C. F. Lai, J. Y. Chi, H. C. Kuo, C. H. Chao, H. T. Hsueh, J.-F. T. Wang, and W. Y. Yeh, "Anisotropy of light extraction from two-dimensional photonic crystals," *Opt. Exp.*, vol. 16, pp. 7285–7294, 2008.

[4] J. J. Wierer, M. R. Krames, J. E. Epler, N. F. Gardner, and M. G. Craford, "InGaN/GaN quantum-well heterostructure light-emitting diodes employing photonic crystal structures," *Appl. Phys. Lett.*, vol. 84, pp. 3885–3887, 2004.

[5] C. F. Lai, J. Y. Chi, H. H. Yen, H. C. Kuo, C. H. Chao, H. T. Hsueh, J.-F. T. Wang, C. Y. Huang, and W. Y. Yeh, "Polarized light emission from photonic crystal light-emitting diodes," *Appl. Phys. Lett.*, vol. 92, pp. 243118-1–243118-3, 2008.

[6] A. David, T. Fujii, B. Moran, S. Nakamura, S. P. DenBaars, C. Weisbuch, and H. Benisty, "Photonic crystal laser lift-off GaN light-emitting diodes," *Appl. Phys. Lett.*, vol. 88, pp. 133514-1–133514-3, 2006.

[7] K. Bergenek, Ch. Wiesmann, R. Wirth, L. O'Faolain, N. Linder, K. Streubel, and T. F. Krauss, "Enhanced light extraction efficiency from AlGaInP thin-film light-emitting diodes with photonic crystals," *Appl. Phys. Lett.*, vol. 93, pp. 041105-1–041105-3, 2008.

[8] M. Yokoyama and S. Noda, "Polarization mode control of two-dimensional photonic crystal laser having a square lattice structure," *IEEE J. Quantum Electron.*, vol. 39, no. 9, pp. 1074–1080, Sep. 2003.

[9] C. F. Lai, J. Y. Chi, H. H. Yen, C. E. Lee, H. C. Kuo, C. H. Chao, H. T. Hsueh, C. Y. Huang, J.-F. T. Wang, W. Y. Yeh, T. C. Lu, and S. C. Wang, "Extraction enhancement and collimation from a thin-film InGaN/GaN photonic crystal light-emitting diodes," in *Proc. '08 SSDM E-10–2*, pp. 988–989.

[10] C. E. Lee, C. F. Lai, Y. C. Lee, H. C. Kuo, T. C. Lu, and S. C. Wang, "Nitride-based thin-film light-emitting diodes with photonic quasi-crystal surface," *IEEE Photon. Technol. Lett.*, vol. 21, pp. 331–333, 2009.

[11] F. S. Diana, A. David, I. Meinel, R. Sharma, C. Weisbuch, S. Nakamura, and P. M. Petroff, "Photonic crystal-assisted light extraction from a colloidal quantum dot/GaN hybrid structure," *Nano Lett.*, vol. 6, pp. 1116–1120, 2006.

[12] A. David, C. Meier, R. Sharma, F. S. Diana, S. P. DenBaars, E. Hu, S. Nakamura, and C. Weisbuch, "Photonic bands in two-dimensionally patterned multimode GaN waveguides for light extraction," *Appl. Phys. Lett.*, vol. 87, pp. 101107-1–101107-3, 2005.

[13] M. F. Schubert, S. Chhajed, J. K. Kim, E. F. Schubert, and J. Cho, "Polarization of light emission by 460 nm GaInN/GaN light-emitting diodes grown on (0001) oriented sapphire substrates," *Appl. Phys. Lett.*, vol. 91, pp. 051117-1–051117-3, 2007.

[14] T. Ochiai and K. Sakoda, "Nearly free-photon approximation for two-dimensional photonic crystal slabs," *Phys. Rev. B*, vol. 64, pp. 045108-1–045108-11, 2001.

[15] V. Pacradouni, W. J. Mandeville, A. R. Cowan, P. Paddon, and J. F. Yong, "Photonic band structure of dielectric membranes periodically textured in two dimensions," *Phys. Rev. B*, vol. 62, pp. 4204–4207, 2000.

Chun-Feng Lai received the M.S. degree in the electro-mechanical engineering from the National Sun Yat-Sen University, Kaohsiung, Taiwan, in 2005. He is currently working toward the Ph.D. degree in the Department of Photonics and Institute of Electro-Optical Engineering, National Chiao Tung University (NCTU), Hsinchu, Taiwan.

His current research interests include high-efficiency GaN-based LED and GaN film-transferred LED via photonic crystals.

Jim-Yong Chi (SM'97) received the B.S. degree in physics from the National Tsinghua University, Hsinchu, Taiwan, in 1971, and the Ph.D. degree in material science from the Massachusetts Institute of Technology, Cambridge, in 1979.

He joined the Industrial Research and Technology Institute, Taiwan, in 1999. He joined the National Dong Hwa University, Hualien, Taiwan, as a Professor and the Director of the Institute of Optoelectronic Engineering in 2008. He was a Member of Technical Staff in Lucent Technologies, Bell Laboratories, GTE Laboratories, Polaroid Corporations, and AMP M/A-COM. He has authored or coauthored more than 200 technical papers and conference papers and has given many invited talks at conferences and institutions.

Dr. Chi won many awards including the 2004 Distinguished Engineers Award by the Association of Chinese Engineers, Taiwan.

Hao-Chung Kuo (S'98–M'99) received the B.S. degree in physics from the National Taiwan University, Taipei, Taiwan, the M.S. degree in electrical and computer engineering from Rutgers University, New Brunswick, NJ, in 1995, and the Ph.D. degree from the Electrical and Computer Engineering Department, University of Illinois at Urbana-Champaign, Urbana-Champaign, in 1999.

During 1993–1995, he was a Research Consultant in Lucent Technologies, Bell Laboratories. During 1999–2001, he was a Member of Technical Staff in Fiber-Optics Division, Agilent Technologies. During 2001–2002, he was with LuxNet Corporation. Since October 2002, he has been with the Institute of Electro-Optical Engineering, National Chiao Tung University (NCTU), Hsinchu, Taiwan, as a Faculty Member. He is currently the Associate Dean, Office of International Affair, NCTU. His current research interests include semiconductor lasers, vertical-cavity surface-emitting lasers (VCSELs), blue and UV LED lasers, quantum-confined optoelectronic structures, optoelectronic materials, and solar cell. He has authored or coauthored 140 internal journal papers, and 6 granted and 10 pending patents.

Prof. Kuo is the IEEE Senior Member and Associate Editor of IEEE/OSA JOURNAL OF LIGHTWAVE TECHNOLOGY and IEEE JOURNAL OF SELECTED TOPICS IN QUANTUM ELECTRONICS (JSTQE)—special issue on Solid-State Lighting. He received Ta-You Wu Young Scholar Award from the National Science Council and Young Photonics researcher award in 2007.

Hsi-Hsuan Yen received the M.S. degree from the Department of Physics, National Central University, Taoyuan, Taiwan, in 2001. He is currently working toward the Ph.D. degree in Department of Photonics and Institute of Electro-Optical Engineering, National Chiao Tung University (NCTU), Hsinchu, Taiwan.

His current research interests include high efficiency GaN-based LED and alternating current GaN-based LED devices.

Chia-En Lee received the B.S. and M.S. degrees in the electrical engineering from the National Chung Hsing University, Taichung, Taiwan, in 2002 and 2004, respectively. He is currently working toward the Ph.D. degree from the Department of Photonics and Institute of Electro-Optical Engineering, National Chiao Tung University (NCTU), Hsinchu, Taiwan.

His current research interests include the nitride-based LEDs.

Chia-Hsin Chao received the B.S.E.E. and Ph.D. degrees from National Sun Yat-Sen University, Kaohsiung, Taiwan, in 1999 and 2006, respectively.

From 2005 to 2006, he was a Visiting Scholar at the Electrical and Computer Engineering Department, University of Illinois at Urbana-Champaign, Urbana-Champaign. From 2006, he has been with Electronic and Opto-Electronics Research Laboratories (EOL), Industrial Technology Research Institute (ITRI), Hsinchu, Taiwan. He is currently a Project Deputy Manager and engaged on photonic crystal LEDs and LED microdisplay. His current research interests include numerical electromagnetic field analysis, photonic crystal, and surface plasmon.

Wen-Yung Yeh received the Ph.D. degree in materials science and engineering from National Tsing Hua University, Hsinchu, Taiwan, in 2001.

He is currently the Deputy Director of the Opto-Electronic Device and System Application Division, Electronics and Opto-Electronics Research Laboratories (EOL), Industrial Technology Research Institute (ITRI), Hsinchu, Taiwan, where he leads the AC LED research team. His current research interests include photonic crystal LED, AC LED, and GaN solar cell.

Dr. Yeh received the R&D 100 Award in 2008.

Tien-Chang Lu received the B.S. degree in electrical engineering from National Taiwan University, Taipei, Taiwan, in 1995, the M.S. degree in electrical engineering from the University of Southern California, Los Angeles, in 1998, and the Ph.D. degree in electrical engineering and computer science from National Chiao Tung University, Hsinchu, Taiwan, in 2004.

Since August 2005, he has been with the Department of Photonics, National Chiao Tung University (NCTU), Hsinchu, Taiwan, as a Faculty Member.